1 Electrodeposition from Ionic Liquids: Interface Processes, Ion Effects, and Macroporous Structures

FRANK ENDRES, NATALIA BORISENKO,
RIHAB AL SALMAN, MOHAMMAD AL ZOUBI,
ALEXANDRA PROWALD, and TIMO CARSTENS
Clausthal University of Technology, Clausthal-Zellerfeld, Germany

SHERIF ZEIN EL ABEDIN
Electrochemistry and Corrosion Laboratory, National Research Centre,
Dokki, Cairo, Egypt

ABSTRACT

In this chapter, we discuss the prospects and challenges of ionic liquids for interfacial electrochemistry and electrodeposition processes. In contrast to aqueous or organic solutions, ionic liquids form surprisingly strongly adhering solvation layers that vary with the applied electrode potential and that alter the tunnelling conditions in a scanning tunnelling microscopy (STM) experiment. Different cation–anion combinations can have an impact on the fundamental electrochemical processes, and the purity of ionic liquids is a key factor in interfacial electrochemistry. It is also shown that ionic liquids have a high potential in the making of three-dimensional ordered macroporous structures of semiconductors.

1.1 INTRODUCTION

Until about the year 2000, most papers dealing with electrochemistry or electrodeposition in or from ionic liquids used systems based on aluminium(III)

Ionic Liquids UnCOILed: Critical Expert Overviews, First Edition. Edited by Natalia V. Plechkova and Kenneth R. Seddon.

chloride and 1,3-dialkylimidazolium ions, which were first reported in 1982 [1]. Although Walden reported in his paper from 1914 [2] on liquids that we often call today "air and water stable ionic liquids," a community of about 10–20 groups worldwide investigated $AlCl_3$-based liquids from 1948 onwards, which can only be handled under the conditions of an inert-gas dry box. One can speculate about the reasons, but one explanation might be that these liquids are (still) relatively easy to produce: mix carefully water-free aluminium(III) chloride with a well-dried organic halide (e.g., 1-butyl-3-methylimidazolium chloride) in a glove box and, depending on the ratio of the components, a Lewis acidic or a Lewis basic liquid is obtained. As aluminium(III) chloride adsorbs and reacts with water, even under the conditions of a dry box, some ageing takes place, which produces less defined oxochloroaluminates(III) by hydrolysis. As aluminium can be easily electrodeposited from these liquids, a common purification method is to perform a refining electrolysis with an aluminium anode and a steel cathode, leading to clear and well-defined electrolytes. A major review on these liquids was written by Hussey [3], and his article well summarises the prospects of these liquids, which were mainly used as electrolytes for the electrodeposition of aluminium and its alloys, and a few other metals [4]. One can say that, in 2000, there seemed to be no more surprises with these liquids and that electrochemical processes seemed to be well understood, except for, maybe, a few unusual observations (mainly reported in meetings), for example, that aluminium deposition is rather problematic if tetraalkylammonium ions are used instead of imidazolium ions. Furthermore, there was practically no understanding of the interfacial electrochemical processes. As these liquids can only be handled under the conditions of a dry box, scanning tunnelling or atomic force microscopy experiments (STM/AFM), which are well suited for such purposes, were extremely demanding. Nevertheless, one of the authors of this chapter (FE) and Freyland showed in a pioneering, but hardly cited, paper [5] that STM experiments can be performed in aluminium(III) chloride-based ionic liquids and that the surface of highly oriented pyrolytic graphite (HOPG) can be resolved atomically. In subsequent papers, it was shown that the surface and the initial deposition steps on Au(111) as a well-defined model surface can be probed in these liquids. Underpotential phenomena that can lead to alloying, sub-monolayer island deposition, and Moiré patterns [6–9] were found. Later results showed that the Au(111) surface seemed to be resolved atomically in a limited potential régime [10]. Although the latter result was a good step forward, the question remained as to why atomic resolution is much more difficult in ionic liquids than in aqueous solutions, where even atomic processes in real time were demonstrated [11].

In 1999, we started with what was considered at that time to be more or less air- and water-stable ionic liquids, namely 1-butyl-3-methylimidazolium hexafluorophosphate, which was home-made. The motivation was clear: aluminium(III) chloride-based liquids were well-defined liquids with many prospects, but the deposition of silicon, germanium, titanium, tantalum, and others was impossible. Either there was a co-deposition/alloying with aluminium or there was no deposition at all, presumably due to the complexing of the precursors. It can be said, open and above board, that our first cyclic voltammogram of [C_4mim][PF_6] on Au(111) was a nightmare: instead of the expected capacitive behaviour (flat line) within an expected electrochemical window of 4 V, a multitude of cathodic and anodic peaks appeared, of which the peaks attributed to chloride (from the synthesis) were still relatively easy to identify. The first STM experiments were also quite disappointing because, in contrast to the nice STM images in the aluminium(III) chloride-based liquids, even the normally easy to probe steps between the gold terraces were hardly seen. Thus, experiments were somehow unexpectedly complicated with these liquids. Without reporting the whole of the story, we found that there are (at least) three requirements for good and reproducible experiments with air- and water-stable ionic liquids: purity, purity, and again purity. With a step-by-step improvement of the quality of the liquid, we could show that the deposition of germanium, silicon, tantalum, Si_xGe_{1-x}, and selenium is possible and that the processes can be well probed on the nanoscale with *in situ* STM. There have been attempts in the literature to deposit magnesium [12–14] and titanium [15], but according to our experience, magnesium has not (yet) been obtained as a pure phase [16], and instead of titanium, titanium sub-halides were obtained [17], and maybe Li-Ti alloys. As discussed in Reference [18], one should not forget that transition and rare earth elements can have a rich chemistry with covalent bonds to non-metallic main group elements. Thus, one should not expect that the electrodeposition of titanium from an ionic liquid is as simple as that of silver from an aqueous solution. Apart from these aspects, we have hitherto encountered several other puzzling phenomena, *inter alia*, which we cannot yet answer successfully:

1. We have not yet succeeded with STM in achieving atomic resolution of Au(111) in air- and water-stable ionic liquids.
2. In some ionic liquids, even HOPG can hardly be probed atomically, although this is quite easy under air with the same device.
3. The electrodeposition of aluminium is influenced by the cation. Even slight modifications in cation structure can alter the grain size of the resulting deposit.
4. The electrodeposition of tantalum from [C_4mpyr][NTf_2] is possible in a narrow potential régime, but much more difficult in [C_4mim][NTf_2].
5. The composition and thickness of electrochemically made Si_xGe_{1-x} is influenced by the ionic liquid species.

A question that we have to address is the following: What would happen if ionic liquids were strongly adsorbed on electrode surfaces, and if this adsorption was different with different liquids?

1.2 RESULTS AND DISCUSSION

1.2.1 Purity Issues

Before our view on electrodeposition processes in or from ionic liquids is discussed, we would like to draw the reader's attention to purity issues. Ten years ago, almost all ionic liquids were synthesised in individual laboratories. With some efforts, the quality of the liquids, and consequently the quality of the experimental results, was quite reproducible. Typical impurities were alkali metal ions (from the precursors), halides, and water. If the liquids were slightly coloured and if this colour interfered with the envisaged application (e.g., spectroscopy), they were purified over silica or alumina to produce clear liquids. At meetings dealing with ionic liquids, companies advertised their products and coloured liquids were criticised by most people, with a few exceptions. Today, there are many companies worldwide that make and sell ionic liquids. The commercial quality is surely much better than five years ago, but there are still some pitfalls. The supplier normally does not tell the consumer how the liquid was made, and in most cases there is no detailed analysis of the liquid. One finds, in the catalogues, purity levels of between 95% and 99%, and the consumer is normally left to interpret without guidance the nature of the 1–5% of whatever. The most pragmatic approach for an experiment is to test if a reaction or a process gives the desired results or not. From the several thousands of papers published in the field of ionic liquids, we dare concluding that a certain impurity level does not seem to alter tremendously organic, inorganic, or technical chemistry reactions (although halide impurities can poison catalytic processes). Even in the electroplating of aluminium, a certain water level does not seem to disturb the result. Can we now conclude that impurities do not generally disturb? Definitely not! In the last five years, many physicists and physical chemists have started fundamental physical experiments both in the bulk and at the interfaces. Due to their extremely low vapour pressures, ionic liquids are suited to ultra-high vacuum (UHV) experiments; for example, they can be studied with photoelectron spectroscopy (X-ray photoelectron spectroscopy [XPS], or ultraviolet photoelectron spectroscopy [UPS]). At a Bunsen Meeting in 2006 at Clausthal University of Technology, Maier and coworkers [19] presented a paper where they reported on silicon at the ionic liquid/UHV interface detected by XPS. The conclusion was that—somehow—during handling, the silicon grease used for sealing the glass flask contaminated the liquid. The paper was published in the journal *Zeitschrift für Physikalische Chemie* and has been well cited to date [19]. For an overview on the prospects of ionic liquids in surface science, we would like to refer to Reference [20]. We ourselves found, by *in situ* STM, that purification with alumina or silica introduces impurities that segregate on the electrode surface and that strongly disturb the image quality and the nanoscale processes [21]. MacFarlane and coworkers confirmed, by dynamic light scattering experiments, that this "purification" process introduces impurities [22].

From our point of view, for surface science experiments, such a post-treatment should be avoided, if possible. We have already found potassium impurities above the 100 ppm level, where the supplier correctly guaranteed for water, halide, and lithium below 10 ppm. When we found potassium, the supplier admitted, after our insistence, that the production process had been changed. In another (also apparently extremely pure) liquid, we found by XPS 10% of a 1,3-dialkylimidazolium salt in [C_4mpyr][NTf_2]. The supplier had no explanation for this observation. From all our experience with the peer-reviewing of papers, we have learnt that the customers often seem to rely "blind" on the suppliers. When we asked the authors to write a few words on the purity, we received comments such as "The liquid was pure within the given limits" or "We know that the impurities mentioned by the referee do not disturb" or "With higher quality liquids, we get exactly the same results," and so on. It is understandable that people want to get their results published in a science system based on international competition, but the question is why there are, for example, contradictory results on the double-layer behaviour of ionic liquids [23–26]. Surely all authors are convinced that they have carried out the best experiments, but what accounts for the different results? We have therefore decided to purchase solely custom-made liquids, where all our experience with the quality of ionic liquids is accounted for. Our recommendation for people interested in fundamental experiments with ionic liquids is the following: start with an extremely pure liquid where all impurities are below 10 ppm. This gives a reliable reference. Then check if the results are the same with lower quality liquids. In surface science in general, and electrochemistry in particular, the approach with low-quality liquids might be dangerous, as the wrong conclusions can be easily drawn. All liquids that we purchase now are subjected to a detailed analytical program. First, we dry them under vacuum at elevated temperature in beakers that were purified with H_2O_2/H_2SO_4 and ultrapure water. Then a cyclic voltammogram is acquired, from which we can already comment on the quality. As the last steps in the analysis, XPS and *in situ* STM experiments are performed. If all these results are convincing, the liquid is cleared for experiments in the laboratory.

1.2.2 Interfacial Layers and Scanning Probe Microscopy Studies

1.2.2.1 AFM Studies When we realised that atomic resolution of Au(111) does not seem to be simple to achieve in air- and water-stable ionic liquids, we wondered what the reason might be for this. An assumption we mentioned at meetings in 2002 and 2003 was that maybe ionic liquids are strongly adsorbed on electrode surfaces, thus delivering a different tunnelling barrier from the one in aqueous solutions. In 2005 and 2006, we investigated the surface of Au(111) in extremely pure [C_4mpyr][NTf_2] and found both a restructuring of the surface [27] and a surface structure that reminded us of the well-known herringbone superstructure known for Au(111). Furthermore, the grain size of electrodeposited aluminium is influenced by the cation, resulting in nanocrystalline aluminium from [C_4mpyr][NTf_2] instead of microcrystalline aluminium from [C_4mim][NTf_2]. We interpreted this surprising result as due to cation adsorption on the electrode surface and the growing nuclei [28]. We should mention that, in the following two years, we were unable to reproduce the results on the herringbone structure. Eventually, we found that some ionic liquid producers scaled up their processes from laboratory scale to pilot plants and that this obviously had an impact on the quality of ionic liquids, at least for experiments at interfaces. One of us (FE) came in touch with the studies performed by Rob Atkin, who showed by scanning force microscopy that ionic liquids are surprisingly strongly adsorbed on the surface of solid materials [29]. Some more papers appeared proving (with different liquids) Atkin's results. At a meeting at Monash University, Atkin and Endres decided to collaborate on experiments on the adsorption of ionic liquids on Au(111). For this purpose, we selected [C_4mpyr][NTf_2] and [C_4mim][NTf_2] from custom syntheses (with all detectable impurities below 10 ppm) to ensure the best possible experiments. The liquids were sealed into ampoules in Clausthal and sent, together with sealed Au(111) samples, to Atkin's laboratory. After a few weeks, Atkin sent us the curves (already evaluated) shown in Figure 1.1. The result is amazing: both liquids are adsorbed on the surface of Au(111), and 3–5 layers can be identified. The results further show that [C_4mpyr][NTf_2] is roughly four times more strongly adsorbed than [C_4mim][NTf_2]. The adsorption of ionic liquids on metal surfaces is, so far, not really surprising, as water and organic solvents are also adsorbed [30–32]; however, the force to rupture these layers is at least one order of magnitude higher than that for water or organic solvents, and a commercial AFM is sufficient for such experiments. This will have an impact on electrochemical processes and on the image quality in STM experiments. A further interesting result is that the ionic liquid/electrode interfacial layer consists of more than one layer. Since an ionic liquid is solvent and solute at the same time, there does not seem to be a simple electrochemical double layer, as concluded from theoretical considerations performed by Kornyshev and Fedorov [33]. The question now arises as to what the STM "sees" at the ionic liquid/electrode interface.

1.2.2.2 **In Situ *STM Studies*** The *in situ* STM allows direct probing of the processes at the electrode/electrolyte interface at different electrode potentials. Although there is a huge community that applies this technique for electrochemical purposes in aqueous solutions, only two other groups (Freyland at Karlsruhe, and Mao at Xiamen) have hitherto published papers on *in situ* STM studies in ionic liquids. One reason might be that the experimental requirements are one order of magnitude more demanding than for aqueous solutions. From our experience, the quality of an ionic liquid can never be good enough for *in situ* STM studies.

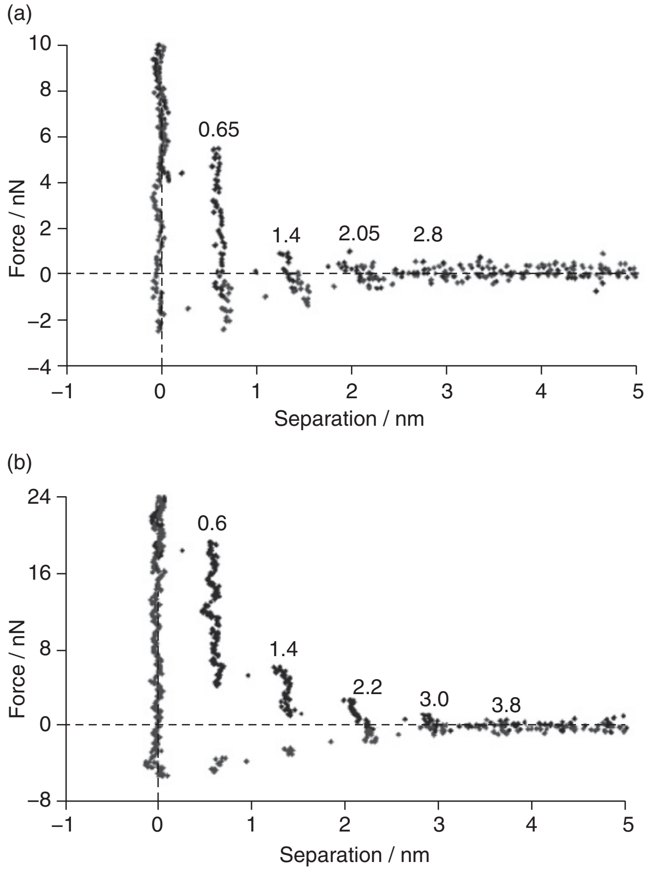

Figure 1.1 (a) Force versus distance profile for an AFM tip (Si_3N_4) approaching and retracting from a Au(111) surface in [C_4mpyr][NTf_2]. At least five steps in the force curve can be seen, extending to a separation of 3.8 nm. The force required to rupture the innermost layer, and move into contact with the gold surface, is 20 nN. The separation distances for each layer prior to push-through are given on the plot. (b) Force versus distance profile for an AFM tip approaching and retracting from a Au(111) surface in [C_4mim][NTf_2]. At least three steps in the force curve can be seen, extending to a separation of 3 nm. The force required to rupture the innermost layer, and move into contact with the gold surface, is 5 nN. The separation distances for each layer prior to push-through are given on the plot.

1.2.3 HOPG/[C_4mpyr][NTf_2]

Let us start with the investigation of the interface between HOPG and [C_4mpyr][NTf_2] (ultrapure liquid from Merck KGaA, Darmstadt, Germany). As already mentioned, it is quite difficult (but not impossible) to probe this surface at atomic resolution. Figure 1.2 shows a cyclic voltammogram of the electrode: the surface oxidation of graphite at the rims starts at moderate

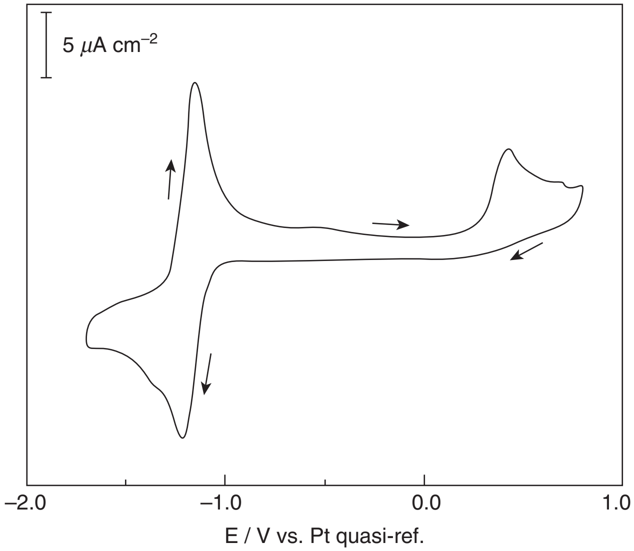

Figure 1.2 Cyclic voltammogram of $[C_4mpyr][NTf_2]$ on HOPG at 25 °C at the scan rate of 10 mV s^{-1}.

potentials of just 0.3–0.4 V. We assume that the peak couple at –1.2 V is due to a surface process. If we now have a look at the interface at the open circuit potential (ocp) (Fig. 1.3a), we identify a flat surface with a defect in the middle. This defect is due to a step consisting of three graphene layers. The surface looks more or less normal, and one would interpret the horizontal stripes as a consequence of a direct tip/surface contact at the step. If we zoom in, however, we clearly see that there is a layer on the surface (Fig. 1.3b), and as a first interpretation one would say this is due to dirt adsorbed to the surface. This interpretation would be tempting and easy, but not understandable, as the liquid is of ultrapure quality. Furthermore, on Au(111), the same liquid does not show such a layer under the same experimental conditions. So, what else can it be? The variation of the electrode potential gives us hints that, at an electrode potential of just 600 mV more in the negative direction, a regular structure appears on the surface which looks hexagonal with a periodicity in the 8- to 10-nm régime (Fig. 1.3c). At slightly more negative electrode potentials, we see a cathodic peak in the cyclic voltammogram. One should not overinterpret such STM images, but from our experience "real" dirt does not give such regular structures upon changing the electrode potential. We can therefore assume that the ionic liquid is subject to a hexagonal superstructure on the hexagonal graphite surface and this reorientation is correlated with an electrochemical response. We can conclude at least that there is a surface layer on top of HOPG that undergoes a reorientation if negative electrode potentials are applied.

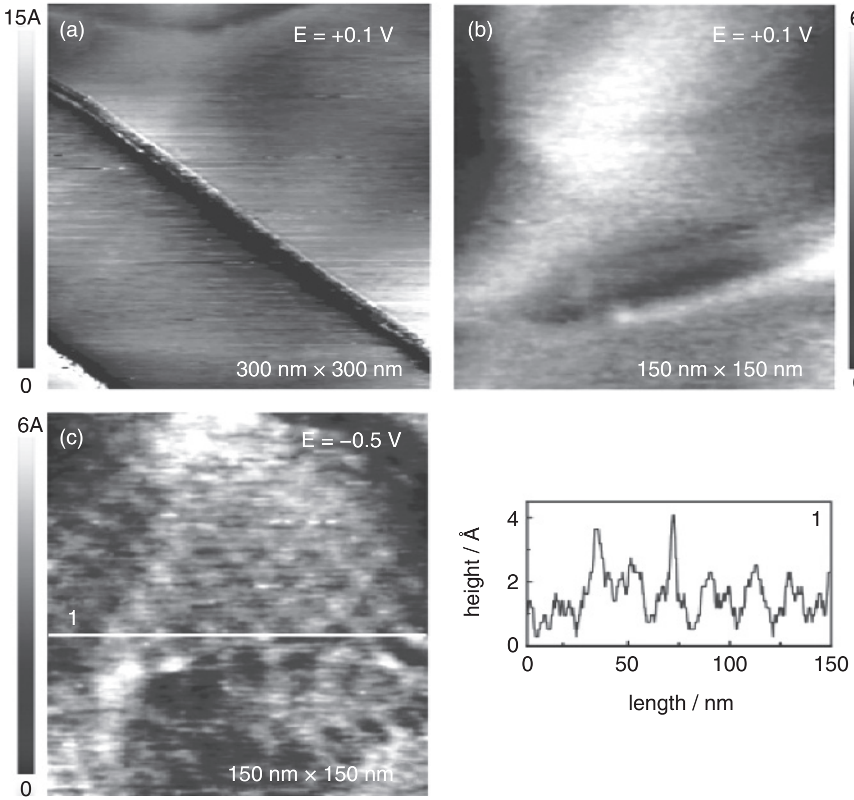

Figure 1.3 A sequence of *in situ* STM images of HOPG in [C_4mpyr][NTf_2]. (a) At +0.1 V versus Pt quasi-reference, a typical surface structure of HOPG is obtained. (b) A higher resolution shows that an adsorbed layer seems to be present. (c) With decreasing electrode potential, a type of an ordering is observed. The individual islands are about 20 nm in width and less than 0.5 nm in height (height profile 1).

1.2.4 Au(111)/[C_6mim][FAP]

Stimulated by a recent paper from Fedorov *et al.* [34], who showed by simulations that the camel shape of the capacitance curve might be due to reorientations at the ionic liquid/electrode interface, we investigated the Au(111) surface under 1-hexyl-3-methylimidazolium tris(pentafluoroethyl)trifluorophosphate ([C_6mim][FAP]). We have had good experiences with this liquid, which can be made in very high quality by Merck. The cyclic voltammogram shown in Figure 1.4 shows only slight peaks within the electrochemical window, and from the electrochemical experiment alone one could only speculate on the surface or bulk processes.

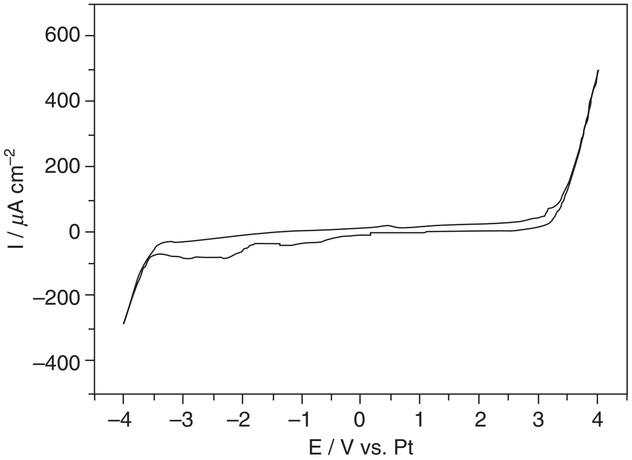

Figure 1.4 Cyclic voltammogram of [C_6mim][FAP] on Au(111) at a scan rate of 10 mV s^{-1}.

The *in situ* STM shows that there are slow processes occurring on the Au(111) surface. Figure 1.5a shows the surface that we obtain in [C_6mim][FAP] under ocp conditions.

The surface shows a wormlike structure with heights of between 200 and 300 pm. We observed a similar surface with [C_4mpyr][NTf_2], whereas with [C_4mim][NTf_2] a rather flat surface was obtained under the same conditions. This result is a hint that the liquid interacts with the surface. If we change the electrode potential to values that are 0.5–1.5 V more negative, a slow reorientation occurs, finally giving a surface with islands on top (Fig. 1.5b). An evaluation of all STM images reveals that the wormlike structures rather merge toform these islands than being the result of a deposition. Interestingly, if we change the electrode potential back to the original value, we do not get the same surface as under ocp conditions. If, on the other hand, we apply initially a potential 0.5–1.5 V more positive than the ocp, we see another restructuring of the surface, as shown in Figure 1.5c. The wormlike surface also transforms slowly, resulting in a differently structured surface. We should mention that all these processes are extremely slow, occurring over hours. This means that the electrochemical experiment alone can be misleading at too high scan rates, and cyclic voltammograms should be acquired with rather slow scan rates, for example, 0.1 mV s^{-1}, if these slow processes are to be probed. However, this will require high-quality instruments to resolve the small currents at low scan rates. Unfortunately, we have so far not yet obtained better quality STM images with this liquid upon zooming in to higher resolution. Furthermore, we have hints that, even with the same liquids, the results are not perfectly reproducible, giving further evidence that even with one and the same liquid, a slightly different outcome cannot be ruled out. In order to shed more light on

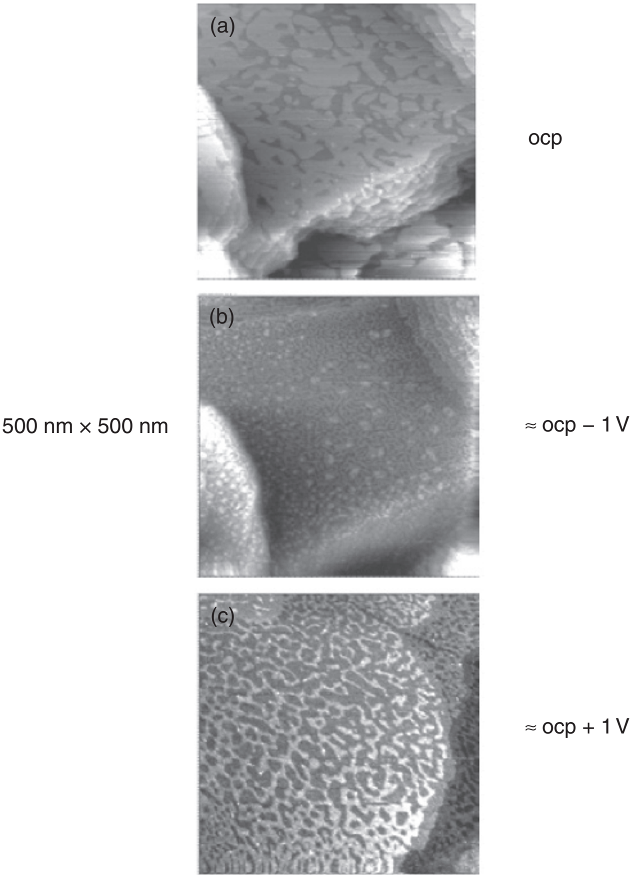

Figure 1.5 *In situ* STM images of Au(111) under [C_6mim][FAP] around the open circuit potential: very slow potential-dependent processes can be observed on the electrode surface.

the STM results with this liquid, we performed tunnelling spectroscopy. This technique is illustrated schematically in Figure 1.6.

In the STM experiment, the distance tip-to-surface is held constant by a feedback circuit after the approach, and in this constant height mode the surface is probed, giving three-dimensional (3D) images of the surface. From the theory of tunnelling, there are now two options to obtain electronic information on the tunnelling process. In one experiment, the feedback circuit is switched off and the tunnelling voltage is varied. The tunnelling current is acquired as a function of the tunnelling voltage, and with the integrated version of Equation (1.1) [35], the tunnelling barrier ϕ can be obtained by fitting the formula to the experimental values:

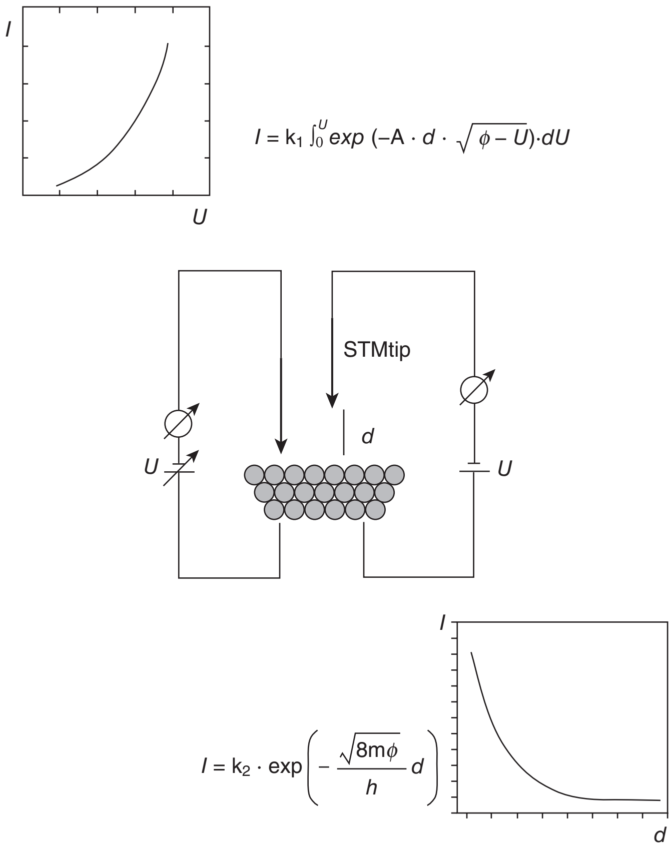

Figure 1.6 A sketch of tunnelling spectroscopy and the formulas behind (see text).

$$I = \mathrm{k}_1 \int_0^U \exp\left(-\mathrm{A} \cdot d \cdot \sqrt{\phi - U}\right) dU \tag{1.1}$$

k_1, A: constants, d: distance, ϕ: tunnelling barrier, U: voltage.

ϕ includes the work functions of tip and electrode, and of other processes involved in the tunnelling. This evaluation has been successfully applied by Zell and Freyland to STM experiments in aluminium(III) chloride-based ionic liquids, and the apparent tunnelling barrier showed a dependence on the alloy composition [36].

Another approach, based on the same theory, is to vary the distance of tip to sample. This can be done by retracting and approaching the tip with the STM scanner. The formula for evaluation is simpler:

$$I = \mathrm{k}_2 \exp\left(-\frac{\sqrt{8m\phi}}{\hbar} d\right) \tag{1.2}$$

k_2: constant, m: electron mass, d: distance.

Here, the apparent tunnelling barrier can be obtained directly from the plot of ln(I) versus d. We prefer this evaluation. On the one hand, there is no need to fit a model to the experimental data. Equation (1.1) requires three variables, that is, k_1, d, and ϕ. On the other hand, that experiment requires a variation of the tip potential, in part over ±1 V, to obtain good enough experimental data. We have, together with Rob Atkin, the first results that these interfacial layers vary with the electrode potential, and consequently the tunnelling barrier might be influenced. With the distance variation, these problems do not occur, and from our experience the results are more reproducible. It might depend on the liquid and the electrode, and thus the experimenter is encouraged to perform both tunnelling spectroscopy experiments to decide. Figure 1.7 shows the evaluated results.

From these data we can conclude, that in this experiment, the tunnelling barrier is lowest around the ocp and rises both to the cathodic and to the anodic régime. We might preliminarily conclude, together with the *in situ* STM results, that the restructuring of the interface leads to a higher tunnelling barrier. It has to be expected that the structure of the ionic liquid's ions will have an influence on the surface processes, and that one should refrain from

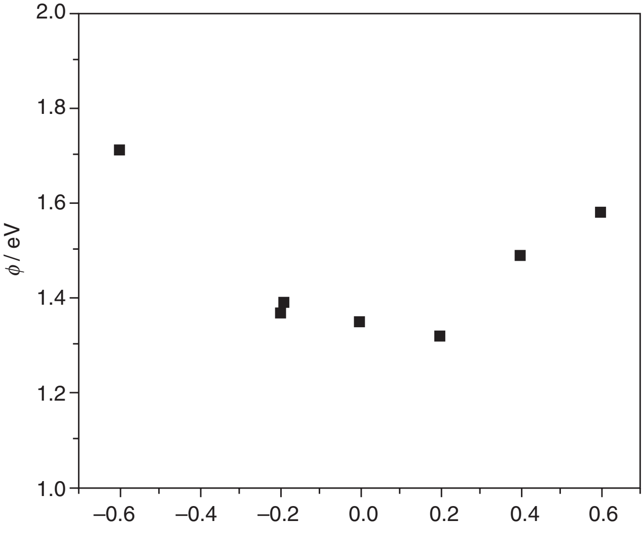

Figure 1.7 The tunnelling barrier of [C_6mim][FAP] /Au(111) at different electrode potentials. The tunnelling barrier has a minimum at the open circuit potential.

extrapolating results from experiments with one liquid/electrode system to another one. In the following section, we show that a variation of the cation can lead to totally different STM results.

1.2.5 Au(111)/[C_4mpyr][FAP]

As already mentioned, we had hints in 2006 that the Au(111)/[C_4mpyr][NTf_2] surface shows, in a certain potential régime, a structure similar to the well-known herringbone superstructure, which has been observed by many groups so far, both under electrochemical conditions and in UHV. As one example, we would like to mention the work of Repain et al. [37]. Unfortunately, we were unable to reproduce our results for two years, and in our experience this was due to a lower liquid quality. Furthermore, we also observed that the bistriflamide can be remarkably unstable under mild electrochemical conditions, and the oxidation of copper in such liquids at elevated temperatures can lead quantitatively to the formation of CuF_2 [38]. For this reason, we selected a liquid of the best possible quality and ordered from Merck a custom synthesis of [C_4mpyr][FAP], together with a detailed analytical protocol. The analysis from Merck showed that all detectable impurities were below 10 ppm. Figure 1.8 shows the cyclic voltammogram of this liquid on Au(111) in the potential régime where the STM experiments were performed.

The platinum (quasi-)reference electrode is not perfect but still a good choice for STM experiments as there are only negligible Faraday currents; thus, the electrode potential remains quite stable. If, however, the electrolyte

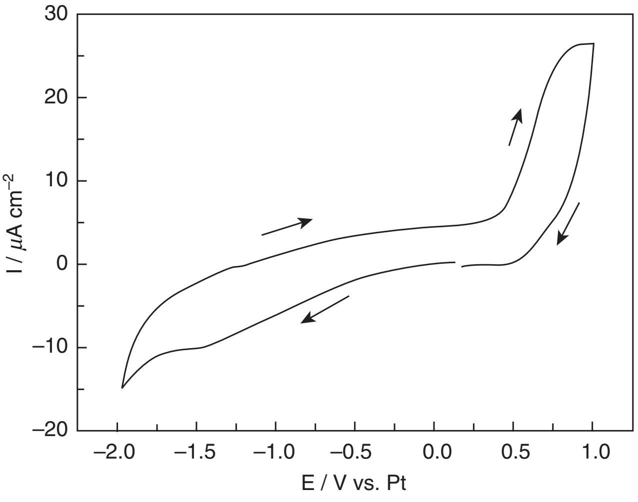

Figure 1.8 Cyclic voltammogram of [C_4mpyr][FAP] on Au(111) in the potential régime from which the STM images of Figure 1.9 were acquired.

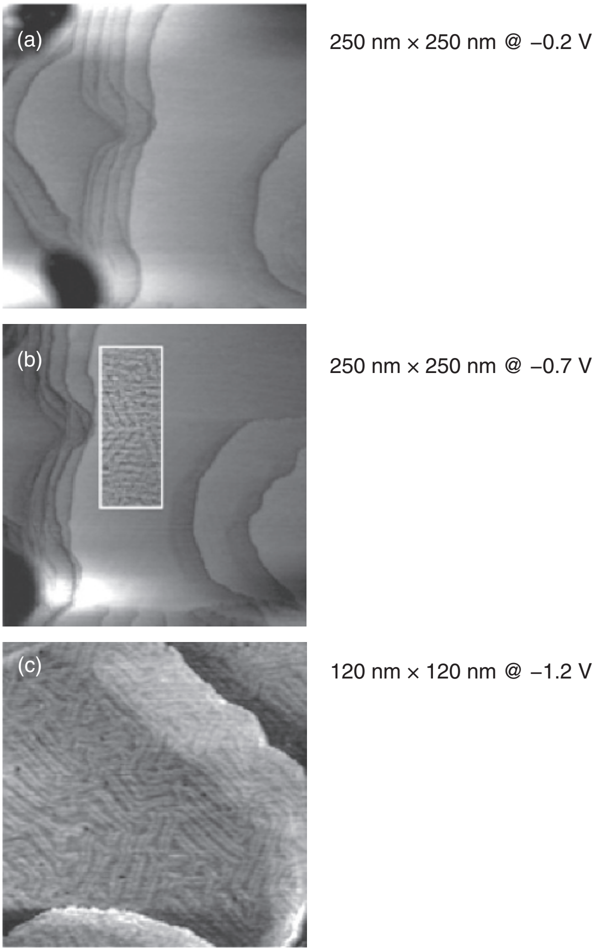

Figure 1.9 *In situ* STM images of Au(111) under [C_4mpyr][FAP]: with decreasing electrode potential, the herringbone superstructure of Au(111) is observed. The inset in (b) shows (with an artificial contrast) the initial herringbone structure.

composition is changed during an experiment, the potential of this electrode will shift by up to 500 mV, depending on the species, in either direction. This quasi-reference electrode can be employed if care is taken, and we employ it since in any case it excludes any side reaction on the electrode surface from reference electrode species. Figure 1.9 shows three *in situ* STM images of Au(111) at different electrode potentials.

At –0.2 V, we see a flat surface. Apart from the typical terraces there is no striking surface structure, even if we zoom in. At –0.7 V, a closer look shows that a structure which is quite similar to the one we observed in 2006 appears [27]. If the electrode potential is further reduced to –1.2 V, and if the resolution is increased to 200 nm × 200 nm, the surface shows a structure that is quite similar to the abovementioned herringbone superstructure. The reported distance between the rims should be 6.4 nm, but one finds slightly varying values in the literature [39, 40]. With a calibrated STM tip, we obtain a value of 5.4 ± 0.5 nm, which is slightly lower than the reported 6.4 nm. The uncertainty arises from the noise in the STM images. If we further zoom in, the STM image becomes a little noisy, but we have hints for the periodic structure of Au(111). Now, the question arises: why in this liquid do we see the herringbone superstructure? We should mention that, in [C_4mim][FAP] of the same quality, we have hitherto not yet seen the herringbone superstructure. Experiments performed in Rob Atkin's laboratory reveal that both liquids are differently adsorbed on Au(111), [C_4mpyr][FAP] more strongly than [C_4mim][FAP], and that the layer thickness varies with the applied electrode potential. The experiments, which will be published separately, show that in the cathodic régime the first layer close to the surface is more compressed compared with the ocp conditions. Preliminary tunnelling spectroscopy experiments performed in our laboratory show that, in the potential régime where the herringbone superstructure is observed, the tunnelling barrier is lowest. All these observations lead us to the preliminary conclusion that, in this limited potential régime, the STM tip is close enough to the surface to allow the electrons to tunnel through the adsorbed ionic liquid layer and make the herringbone structure visible. Maybe it is just a small step now, in this liquid, to probing the surface with atomic resolution. However, this does not mean that this aim can be achieved in all liquids easily. So far, we have not yet seen the herringbone structure with [C_4mim][FAP], and at least we can conclude that other electrochemical and tunnelling parameters are required. In contrast to *in situ* STM experiments in water, ionic liquids are much more challenging. Not only the purity plays a rôle, but there is also a dependence on the ions and solutes added (e.g., for the sake of electrodeposition) to ionic liquids, which might again change the interface structure. These studies are in their infancy, but there is an increased awareness now, and more and more people are starting to realise that it is not just the electrochemical window that makes ionic liquids interesting for electrochemical purposes. With a fundamental understanding of the interfacial processes, there is also a great chance of developing tailored technical processes.

1.2.6 Influence of the Cation on Aluminium Deposition

When we started with experiments on the electrodeposition of aluminium from air- and water-stable ionic liquids, we had quite a simple motivation to use [C_4mpyr][NTf_2]. This liquid can be well dried below 3 ppm H_2O. If dry aluminium(III) chloride is added, there is no risk of a reaction with water which, in contrast, is almost unavoidable if aluminium(III) chloride is mixed with, for example, [C_4mim]Cl, which is quite difficult to dry. Another reason was that we planned pulsed electrodeposition to make nanocrystalline aluminium deposits, and we expected a wider electrochemical window for $[C_4mpyr][NTf_2]$ compared with $[C_4mim][NTf_2]$. It was a great surprise when we realised, after the first set of experiments, that even under potentiostatic conditions with not that high overvoltages, reproducibly nanocrystalline aluminium was obtained [41]. Control experiments showed that with $[C_4mim][NTf_2]$ under quite similar experimental conditions, microcrystalline aluminium deposits were obtained [28]. We could exclude viscosity effects. An *in situ* STM study showed that there were more differences between the liquids: we found an underpotential deposition of aluminium and a surface alloy Al/Au in $[C_4mim][NTf_2]$, but not in $[C_4mpyr][NTf_2]$. Later, we showed that the electroactive species in both liquids are identical [42]. Only one explanation remained: the cation of the liquid influences the deposition process and from Atkin's AFM measurements, it is likely that the $[C_4mpyr]^+$ ion behaves like a surface-active species. We found more surprising effects. If the $[C_4mim]^+$ ion is electrochemically decomposed prior to deposition experiments, again nanocrystalline aluminium is obtained. From all these results, we can conclude, at least, that the cation (and likely also the anion) of ionic liquids influences the electrodeposition process. Presumably, the interfacial layers play a rôle, but a close insight would require not only STM and AFM experiments, but also other surface-sensitive techniques, such as sum-frequency generation spectroscopy experiments under electrochemical control. In the following, we would like to show that even variations in the cation structure can lead to surprising results. Together with a company, we investigated the aluminium deposition from a mixture of aluminium(III) chloride with 1-(2-methoxyethyl)-3-methylimidazolium chloride [43].

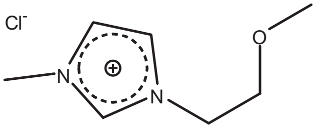

Structural formula of 1-(2-methoxyethyl)-3-methylimidazolium chloride

The cyclic voltammogram was normal, showing a reversible aluminium deposition/stripping (Fig. 1.10). Surprisingly, the deposit was semi-bright from the beginning, and the SEM analysis (as well as an X-ray powder diffraction [XRD] analysis) showed nanocrystals instead of the expected microcrystals (Fig. 1.11).

We tested other organic halides with two ether groups in the imidazolium side chain, and again we obtained different results: in part we only found black deposits, although there was no hint of the decomposition of the liquid.

All our experiences with electrodeposition from ionic liquids lead us to the following conclusion: not only does the electroactive species play a rôle, but even slight variations in the cation and/or anion structure may also have an

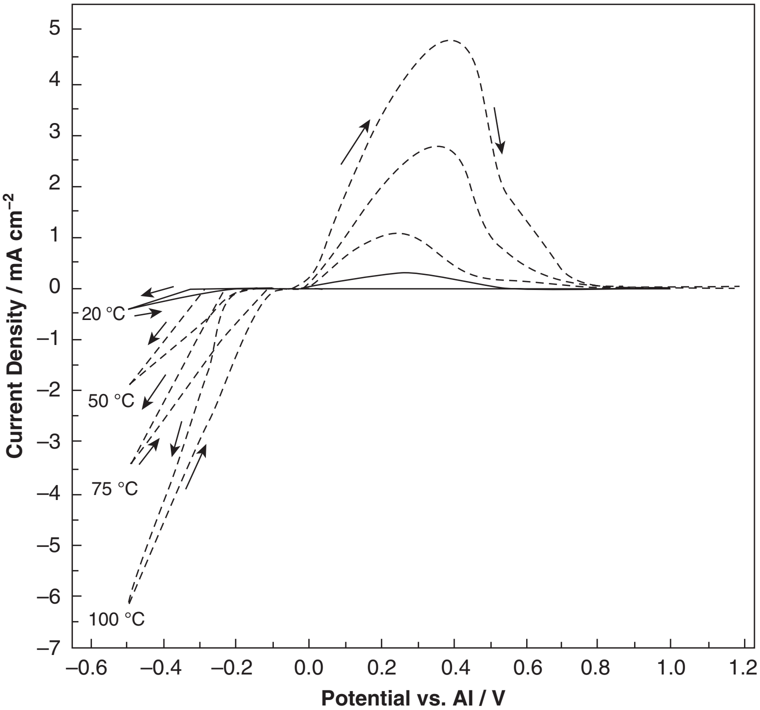

Figure 1.10 Temperature-dependent cyclic voltammograms of aluminium deposition from 1-(2-methoxyethyl)-3-methylimidazolium chloride/aluminium(III) chloride.

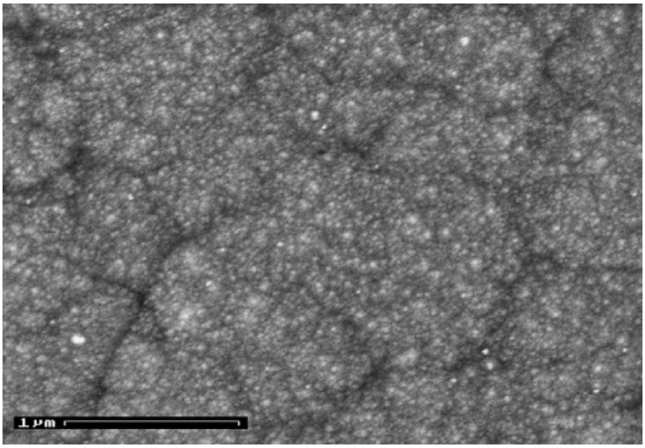

Figure 1.11 Nanocrystalline aluminium deposited from 1-(2-methoxyethyl)-3-methylimidazolium chloride/aluminium(III) chloride.

effect. As ionic liquids are definitely (and different strongly) adsorbed onto electrode surfaces, we assume that the interfacial layers influence the elemental electrochemical processes. Interfacial layers will, according to our experience, be influenced both by the solute and by impurities, and there might be time dependent effects. One should **definitely** not expect that all liquids behave in the same manner.

1.2.7 Challenges in the Making of Macroporous Materials

In the past three years, we have expanded our activities to the template-assisted electrodeposition of nanomaterials. These activities involve the electrodeposition of nanowires (silicon, SiGe, and silver), and of macroporous materials. For nanowires, we employ commercial membranes with a defined pore size in which the deposition is performed; in the case of macroporous materials, we deposit polystyrene spheres on the surface of the electrode and fill the voids by electrodeposition. After dissolution of the polystyrene spheres, we get a replica. Figure 1.12 shows a sketch of the electrodeposition principle.

In contrast to the numerous, and mainly nonreproducible, literature data, we apply the polystyrene spheres by simply dipping the electrode into an alcoholic suspension of commercial polystyrene spheres. Upon retracting from the suspension, the alcohol evaporates and a well-ordered 3D polystyrene opal structure is obtained (Fig. 1.13).

On flat surfaces in particular, we get well-ordered polystyrene layers up to 10-μm thick with ordered islands that have lateral dimensions of up to 20 μm × 20 μm. We should mention that how well the spheres self-assemble not only depends on the surface roughness, but also depends on the material. So far we have obtained our best quality samples with gold single crystals, but also indium-tin oxide (ITO) can be employed as a substrate for polystyrene precipitation. We could show that photonic crystals of germanium can be made by electrodeposition and that this material exhibits optical band gap behaviour [44]. A typical structure and a typical optical behaviour are shown in Figure 1.14.

Due to the low surface tension, the ionic liquid easily wets the electrode surface underneath the polystyrene spheres, and germanium grows from the bottom to the top quite regularly. We could now say that it is trivial to make such 3D ordered macroporous (3DOM) substrates, and germanium photonic crystals are indeed easy to make. But it is not that simple. Apart from germanium, there are other materials that are interesting, if macroporous. 3DOM silicon, for example, has a high potential for radio frequency applications. Macroporous aluminium and its alloys would be interesting as anode host materials in lithium ion batteries [45]; 3DOM conducting polymers and noble metals have a high potential in catalysis; and so on. However, Figure 1.15 shows that one has to be prepared for surprises when attempting to make 3DOM materials from ionic liquids.

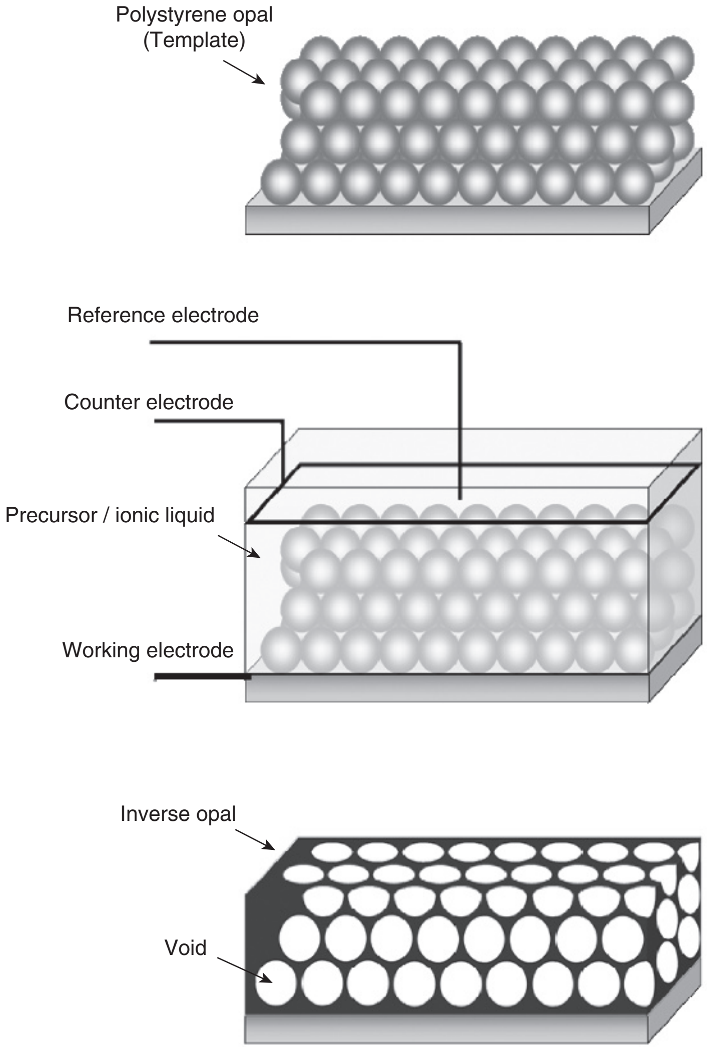

Figure 1.12 Schematic illustration of the electrochemical synthesis of macroporous materials from ionic liquids. Top: A template of polystyrene (PS) on a conducting substrate. Middle: Electrochemical cell. Bottom: Inverse opal of the deposited material after removal of the template by tetrahydrofuran.

The first scanning electron microscopy (SEM) pictures show attempts to make 3DOM silicon by potentiostatic electrodeposition, followed by removal of the polystyrene spheres. In contrast to 3DOM–Ge, there is no such long range regular structure and a disintegration of the polystyrene template during electrodeposition has obviously occurred. The growth processes of silicon and germanium are different, and also influenced by the ionic liquid itself. An

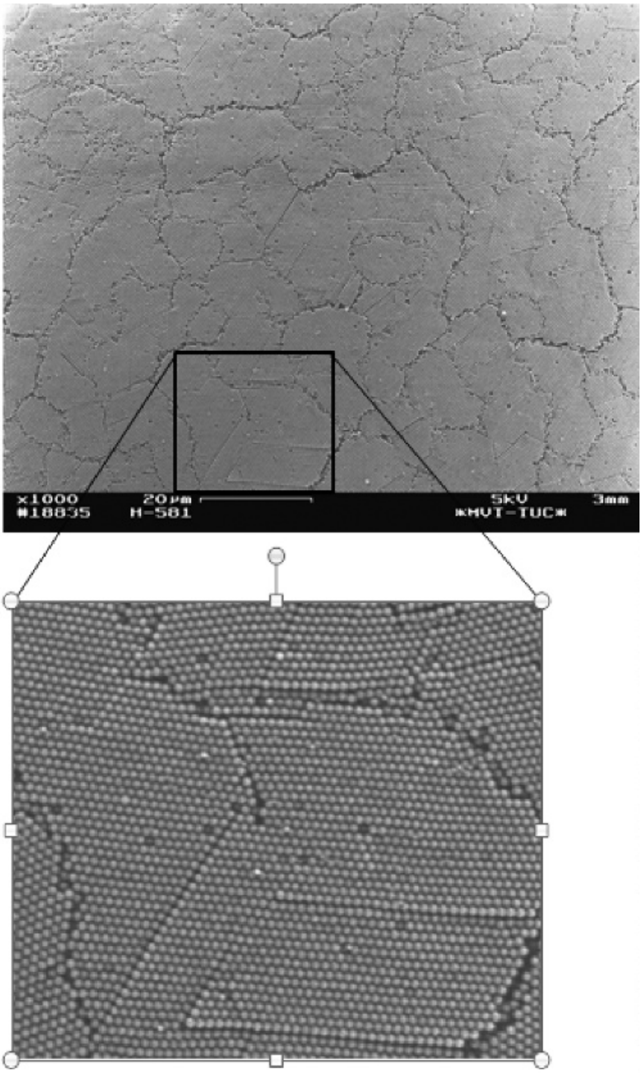

Figure 1.13 Gold thin film (cleaned with limonene) coated with hexagonally ordered polystyrene spheres (diameter 581 nm from Duke Scientific, Palo Alto, CA, USA). For SEM imaging, the template was slightly annealed for 2 hours at 70 °C.

ordered growth of 3DOM–Si will presumably require other parameters. Whereas the deposition of 3DOM–Al on a polished copper electrode from $[C_4mim]Cl\text{-}AlCl_3$ is relatively easy to control [45], the deposition on ITO under similar conditions is more complicated and can lead to structures such as shown in Figure 1.15. A controlled growth with the aim of making 3DOM–Al on ITO requires well-adapted electrochemical parameters.

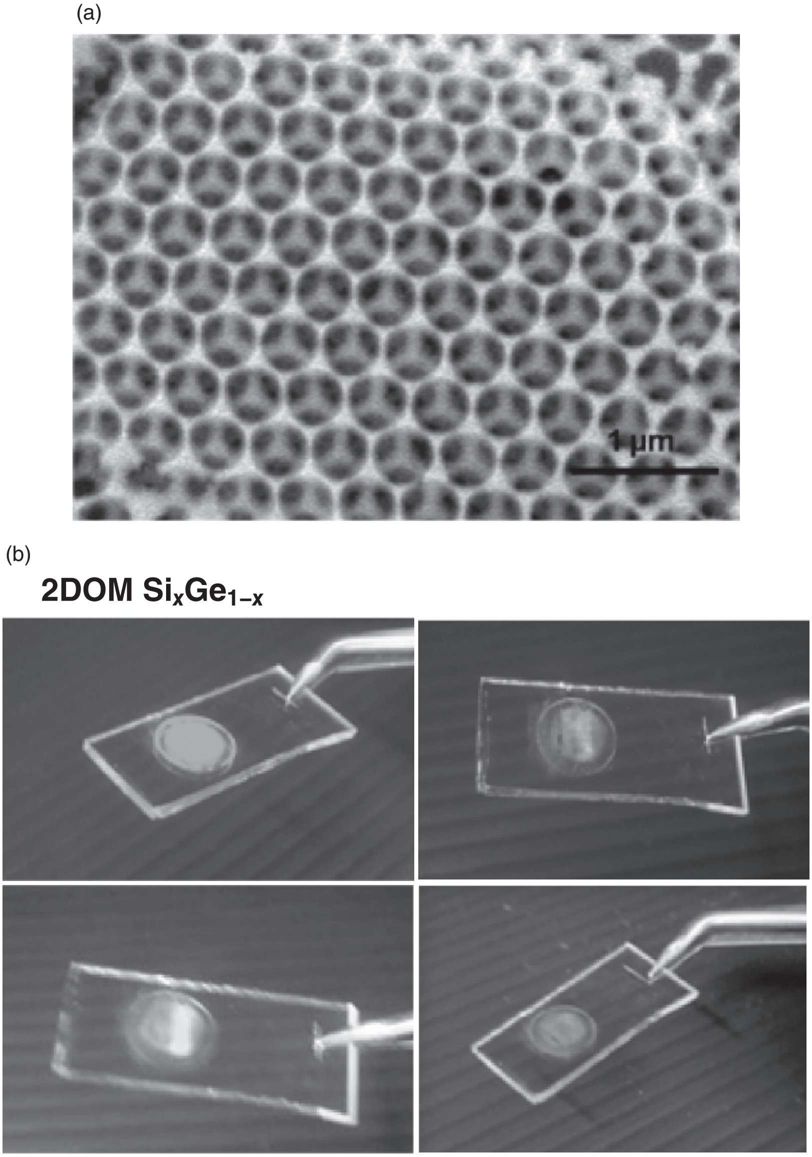

Figure 1.14 (a) SEM image of 3DOM Ge on ITO-glass after removal of the polystyrene template (370 nm), obtained potentiostatically at –2.1 V (vs. Ag quasi-reference electrode) for 30 minutes. 0.1 M $GeCl_4$ in $[C_4mim][NTf_2]$. (b) Photographs of 2DOM Si_xGe_{1-x} (pore size ~370 nm) on ITO–glass substrate showing a colour change with changing the angle of the incident visible white light ($GeCl_4$ + $SiCl_4$) (0.1 + 0.1 M) in $[C_4mim][NTf_2]$. See colour insert.

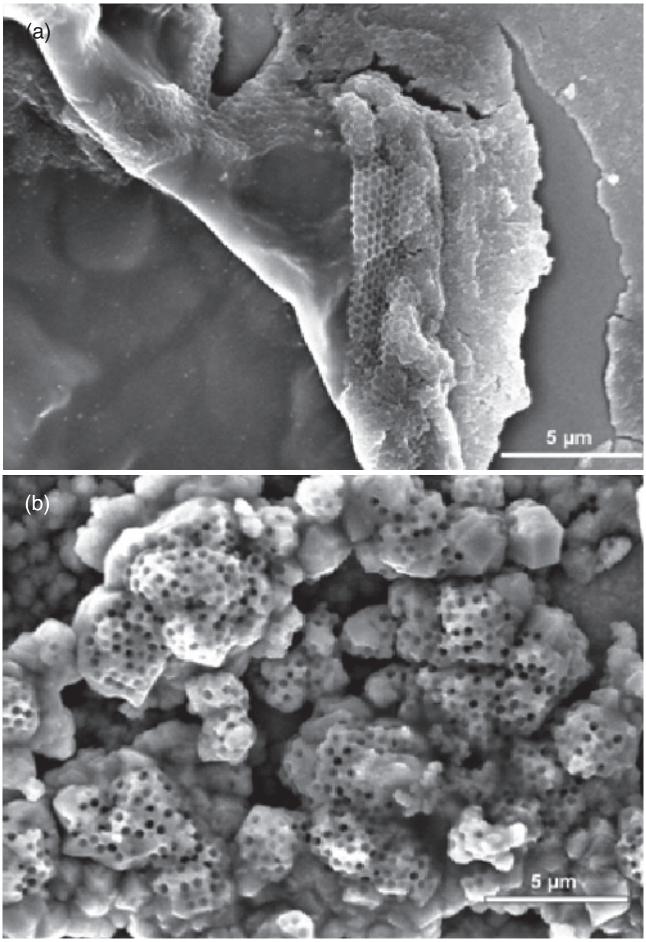

Figure 1.15 (a) Less successful approaches: SEM images of attempted macroporous silicon obtained after overpotential deposition (0.3 M $SiCl_4$ in $[C_4mpyr][FAP]$) for 1 hour, followed by removal of the polystyrene template (400 nm). (b) SEM images of irregular macroporous aluminium from $[C_4mim]Cl\text{-}AlCl_3$ on ITO–glass substrates: with a too fast growth, the polystyrene template is corrupted and an irregular structure results.

1.3 CONCLUSION

This chapter has shown that electrochemical reactions in ionic liquids are considerably different from those in aqueous solutions. Ionic liquids form remarkably strongly adherent interfacial layers on electrode surfaces, and the adsorption varies with the composition of the liquid and with the applied electrode potential. Furthermore, the surface chemistry is strongly dependent on the quality of the liquid, and from our point of view for fundamental physicochemical and electrochemical experiments, the quality of the liquid cannot be high enough. Our *in situ* STM experiments have shown that the surface chemistry is influenced by the ionic liquid and that even slight changes in cation–anion combination have an effect. In a limited potential régime, the herringbone superstructure of Au(111) is visible in [C_4mpyr][FAP], and maybe it is not a too long way to go to achieve atomic resolution in this liquid. In other liquids, such as [C_4mim][FAP] or [C_6mim][FAP], we have not yet observed this nice superstructure. Results from Atkin's group make it likely that the thickness of the interfacial layers, and maybe their structures, vary with the electrode potential and with the liquid itself, and that in each liquid individual tunnelling parameters have to be found for STM experiments. It is furthermore likely that these interfacial layers influence the electrodeposition process, and even slight modifications such as the introduction of an ether group alter, for example, the grain size of deposited aluminium. Apart from these very fundamental aspects, which are still in their infancy, ionic liquids have the potential to make functional materials with macroporous structures, and photonic crystals. In our opinion, electrochemical processes in ionic liquids are not yet straightforward, and many more fundamental studies will be required.

REFERENCES

1 Wilkes, J.S., Levisky, J.A., Wilson, R.A., and Hussey, C.L., Dialkylimidazolium chloroaluminate melts—a new class of room-temperature ionic liquids for electrochemistry, spectroscopy, and synthesis, *Inorg. Chem.* **21**, 1263–1264 (1982).

2 Walden, P., Über die Molekulargrösse und elektrische Leitfähigkeit einiger geschmolzenen Salze, *Bull. Acad. Impér. Sci. St. Pétersbourg* **8**, 405–422 (1914).

3 Hussey, C.L., Room temperature molten salt systems, in: *Advances in molten salt chemistry*, Vol. 5, ed. G. Mamantov, Elsevier, New York (1983), pp. 185–230.

4 Endres, F., Ionic liquids: solvents for the electrodeposition of metals and semiconductors, *Chemphyschem* **3**, 144–154 (2002).

5 Endres, F., Freyland, W., and Gilbert, B., Electrochemical scanning tunnelling microscopy (EC-STM) study of silver electrodeposition from a room temperature molten salt, *Ber. Bunsenges. Phys. Chem.* **101**, 1075–1077 (1997).

6 Moustafa, E.M., Zein El Abedin, S., Shkurankov, A., Zschippang, E., Saad, A.Y., Bund, A., and Endres, F., Electrodeposition of Al in 1-butyl-1-methylpyrrolidinium bis(trifluoromethylsulfonyl)amide and 1-ethyl-3-methylimidazolium bis(trifluoromethylsulfonyl)amide ionic liquids: in situ STM and EQCM studies, *J. Phys. Chem. B* **111**, 4693–4704 (2007).

7 Freyland, W., Zell, C.A., Zein El Abedin, S., and Endres, F., Nanoscale electrodeposition of metals and semiconductors from ionic liquids, *Electrochim. Acta* **84**, 3053–3061 (2003).

8 Mann, O., and Freyland, W., Mechanism of formation and electronic structure of semiconducting ZnSb nanoclusters electrodeposited from an ionic liquid, *Electrochim. Acta* **53**, 514–524 (2007).

9 Wang, F.-X., Pan, G.-B., Liu, Y.-D., and Xiao, Y., Pb deposition onto Au(111) from acidic chloroaluminate ionic liquid, *Chem. Phys. Lett.* **488**, 112–115 (2010).

10 Pan, G.-B., and Freyland, W., 2D phase transition of PF_6 adlayers at the electrified ionic liquid/Au(111) interface, *Chem. Phys. Lett.* **427**, 96–100 (2006).

11 Magnussen, O.M., Zitzler, L., Gleich, B., Vogt, M.R., and Behm, R.J., In-situ atomic-scale studies of the mechanisms and dynamics of metal dissolution by high-speed STM, *Electrochim. Acta* **46**, 3725–3733 (2001).

12 NuLi, Y., Yang, J., and Wang, P., Electrodeposition of magnesium film from $BMIMBF_4$ ionic liquid, *Appl. Surf. Sci.* **252**, 8086–8090 (2006).

13 Wang, P., NuLi, Y., Yang, J., and Feng, Z., Mixed ionic liquids as electrolyte for reversible deposition and dissolution of magnesium, *Surf. Coat. Technol.* **201**, 3783–3787 (2006).

14 Feng, Z., NuLi, Y., Wang, J., and Yang, J., Study of key factors influencing electrochemical reversibility of magnesium deposition and dissolution, *J. Electrochem. Soc.* **135**, C689–C693 (2006).

15 Mukhopadhyay, I., Aravinda, C.L., Borissov, D., and Freyland, W., Electrodeposition of Ti from $TiCl_4$ in the ionic liquid l-methyl-3-butyl-imidazolium bis(trifluoromethylsulfone)imide at room temperature: study on phase formation by in situ electrochemical scanning tunneling microscopy, *Electrochim. Acta* **50**, 1275–1281 (2005).

16 Cheek, G.T., O'Grady, W.E., Zein El Abedin, S., Moustafa, E.M., and Endres, F., Electrochemical studies of magnesium deposition in ionic liquids, *J. Electrochem. Soc.* **155**, D91–D95 (2008).

17 Endres, F., Zein El Abedin, S., Saad, A.Y., Moustafa, E.M., Borisenko, N., Price, W.E., Wallace, G.G., MacFarlane, D.R., Newman, P.J., and Bund, A., On the electrodepsoition of tantalum in ionic liquids, *Phys. Chem. Chem. Phys.* **10**, 2189–2199 (2008).

18 Schubert, T., Zein El Abedin, S., Abbott, A.P., McKenzie, K.J., Ryder, K.S., and Endres, F., Electrodeposition of metals, in: *Electrodeposition from ionic liquids*, eds. F. Endres, D.R. MacFarlane, and A.P. Abbott, Wiley-VCH, Weinheim (2008), pp. 83–123.

19 Gottfried, J.M., Maier, F., Rossa, J., Gerhard, D., Schulz, P.S., Wasserscheid, P., and Steinrück, H.-P., Surface studies on the ionic liquid 1-ethyl-3-methylimidazolium ethylsulfate using X-ray photoelectron spectroscopy (XPS), *Z. Phys. Chem.* **220**, 1439–1453 (2006).

20 Steinrück, H.-P., Surface science goes liquid, *Surf. Sci.* **604**, 481–484 (2010).

21 Endres, F., Zein El Abedin, S., and Borisenko, N., Probing of lithium and alumina impurities in air- and water stable ionic liquids by cyclic voltammetry and in situ scanning tunnelling microscopy, *Z. Phys. Chem.* **220**, 1377–1394 (2006).

22 Clare, B.R., Bayley, P.M., Best, A.S., Forsyth, M., and MacFarlane, D.R., Purification or contamination? The effect of sorbents on ionic liquids, *Chem. Comm.* 23, 2689–2691 (2008).

23 Su, Y.-Z., Fu, Y.-C., Yan, J.-W., Chen, Z.-B., and Mao, B.-W., Double layer of Au(100)/ionic liquid interface and its stability in imidazolium-based ionic liquids, *Angew. Chem. Int. Ed. Engl.* **48**, 5148–5151 (2009).

24 Alam, M.T., Islam, M.M., Okajima, T., and Ohsaka, T., Measurements of differential capacitance in room temperature ionic liquid at mercury, glassy carbon and gold electrode interfaces, *Electrochem. Commun.* **9**, 2370–2374 (2007).

25 Islam, M.M., Alam, M.T., and Ohsaka, T., Electrical double-layer structure in ionic liquids: a corroboration of the theoretical model by experimental results, *J. Phys. Chem. C* **112**, 16568–16574 (2008).

26 Gnahm, M., Pajkossy, T., and Kolb, D.M., The interface between Au(111) and an ionic liquid, *Electrochim. Acta* **55**, 6212–6217 (2010).

27 Borisenko, N., Zein El Abedin, S., and Endres, F., In situ investigation of gold reconstruction and of silicon electrodeposition in the room temperature ionic liquid 1-butyl-1-methylpyrrolidinium bis(trifluoromethylsulfonyl)imide, *J. Phys. Chem. B* **110**, 6250–6256 (2006).

28 Zein El Abedin, S., Moustafa, E.M., Hempelmann, R., Natter, H., and Endres, F., Electrodeposition of nano- and microcrystalline aluminium in some water and air stable ionic liquids, *ChemPhysChem* **7**, 1535–1543 (2006).

29 Atkin, R., and Warr, G.G., Structure in confined room-temperature ionic liquids, *J. Phys. Chem. C* **111**, 5162–5168 (2007).

30 O’Shea, S.J., Welland, M.E., and Pethica, J.B., Atomic force microscopy of local compliance at solid-liquid interfaces, *Chem. Phys. Lett.* **223**, 336–340 (1994).

31 Lim, R., and O’Shea, S.J., Discrete solvation layering in confined binary liquids, *Langmuir* **20**, 4916–4919 (2004).

32 Jeffery, S., Hoffmann, P.M., Pethica, J.B., Ramanujan, C., Ozer, H.O., and Oral, A., Direct measurement of molecular stiffness and damping in confined water layers, *Phys. Rev. B* **70**, 054114 (2004).

33 Fedorov, M.V., and Kornyshev, A.A., Ionic liquid near a charged wall: structure and capacitance of electrical double layer, *J. Phys. Chem. B* **112**, 11868–11872 (2008).

34 Fedorov, M.V., Georgi, N., and Kornyshev, A.A., Double layer in ionic liquids: the nature of the camel shape of capacitance, *Electrochem. Commun.* **12**, 296–299 (2010).

35 Hamers, R.J., Tunneling Spectroscopy, in: *Scanning tunneling microscopy and spectroscopy: theory, techniques and applications*, ed. D.A. Bonnell, Wiley-VCH, New York (1993), pp. 51–103.

36 Zell, C.A., and Freyland, W., In situ STM and STS study of Co and Co-Al alloy electrodeposition from an ionic liquid, *Langmuir* **19**, 7445–7450 (2003).

37 Repain, V., Berroir, J.M., Rousset, S., and Lecoeur, J., Reconstruction, step edges and self-organization on the Au(111) surface, *Appl. Surf. Sci.* **162**, 30–36 (2000).

38 Ismail, A.S., Zein El Abedin, S., Höfft, O., and Endres, F., Unexpected decomposition of the bis(trifluoromethylsulfonyl) amid anion during electrochemical copper oxidation in an ionic liquid, *Electrochem. Commun.* **12**, 909–911 (2010).

39 Hasegawa, Y., and Avouris, P., Manipulation of the reconstruction of the Au(111) surface with the STM, *Science* **258**, 1763–1765 (1992).

40 Oka, H., and Sueoka, K., Connection of herringbone ridges on reconstructed Au(111) surfaces observed by scanning tunneling microscopy, *Jpn. J. Appl. Phys.* **44**, 5430–5433 (2005).

41 Zein El Abedin, S., Moustafa, E.M., Hempelmann, R., Natter, H., and Endres, F., Additive free electrodeposition of nanocrystalline aluminium in a water and air stable ionic liquid, *Electrochem. Commun.* **7**, 1116–1121 (2005).

42 Eiden, P., Liu, Q.X., Zein El Abedin, S., Endres, F., and Krossing, I., An experimental and theoretical study of the aluminium species present in $AlCl_3$/[BMP]Tf_2N and $AlCl_3$/[EMIm]Tf_2N ionic liquids, *Chem. Eur. J.* **15**, 3426–3434 (2009).

43 Zein El Abedin, S., Giridhar, P., Schwab, P., and Endres, F., Electrodeposition of nanocrystalline aluminium from a chloroaluminate ionic liquid, *Electrochem. Commun.* **12**, 1084–1086 (2010).

44 Meng, X., Al-Salman, R., Zhao, J., Borissenko, N., Li, Y., and Endres, F., Electrodeposition of 3D ordered macroporous germanium from ionic liquids: a feasible method to make photonic crystals with a high dielectric constant, *Angew. Chem. Int. Ed. Engl.* **48**, 2703–2707 (2009).

45 Gasparotto, L.H.S., Prowald, A., Borisenko, N., Zein El Abedin, S., and Endres, F., Electrochemical synthesis of macroporous aluminium: a possible host anode material for rechargeable Li-ion batteries, *J. Power Sources* **196**, 2879–2883 (2011).